SUPPLEMENTARY DATA

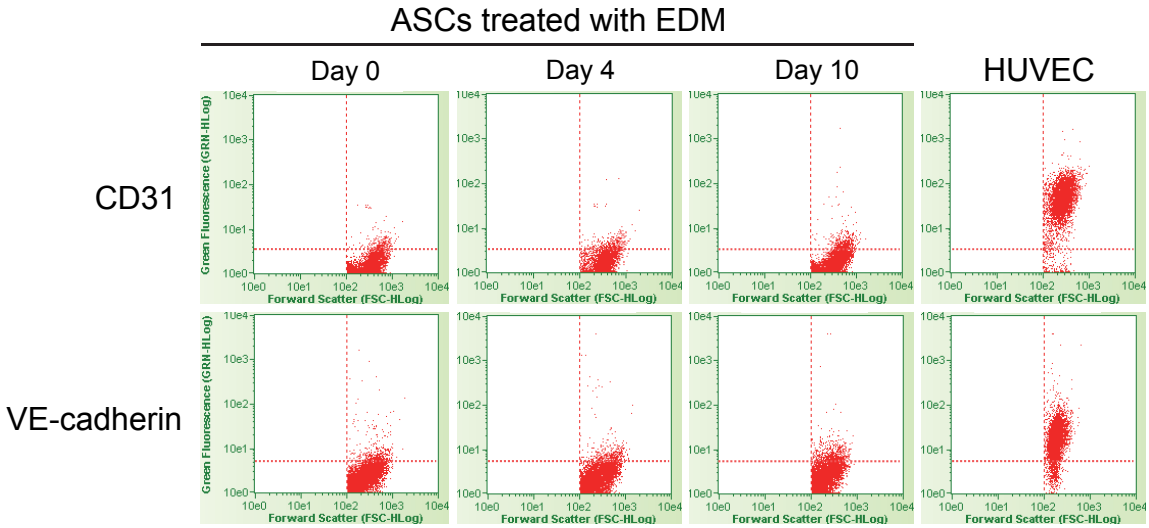

Figure S1. Endothelial cell differentiation of ASC. ASCs were incubated in EDM for the indicated days. The proportion of CD31 or VE-cadherin positive cells was determined using immunocytochemistry and flow cytometry analysis. HUVEC was used as a positive control.

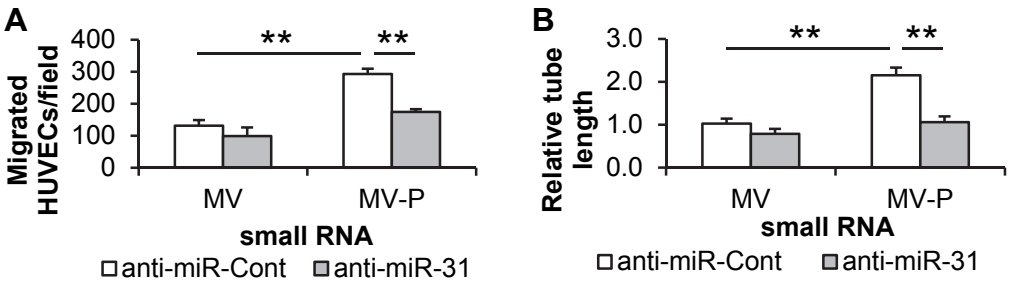

Figure S2. MiR-31 contributes to the proangiogenesis as an effective factor in small RNA from MV-P. Co-transfection of 0.5 μg/ml of small RNA extracted from MV or MV-P with 10 nM of anti-miR-31 was performed in the HUVECs. Anti-miR-Cont was used as a control of anti-miR-31. HUVEC migration **(A)** and tube formation **(B)** were examined. (n = 3 – 5, $^{**}P < 0.01$).

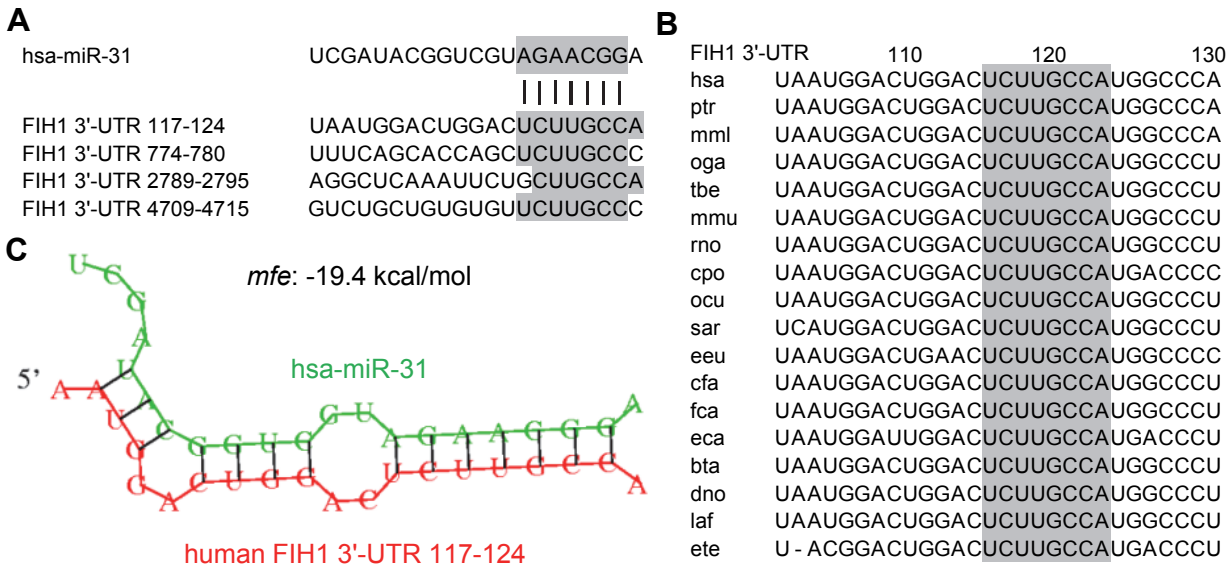

Figure S3. MiR-31 and its conserved binding sites at FIH1 3'-UTR. **(A)** There are four predicted miR-31 targets at 3'-UTR of FIH1. **(B)** Only the one with binding site at 117-224 is broadly conserved among vertebrates. **(C)** The minimum free energy (*mfe*) between hsa-miR-31 and human FIH1 3'-UTR at the site of 117-124 was calculated using the PicTar open-source software.

Rank	microRNA
1	miR-1262
2	miR-549
3	miR-1274B
4	miR-222
5	miR-1274A
6	miR-1267
7	miR-99a
8	miR-100
9	miR-720
10	miR-17
11	miR-24
12	miR-31
13	miR-106a
14	miR-19b
15	miR-221

Table S1. Top 15 abundant miRNAs in ASC-released MV-P based on the miRNA array analysis. Detailed information can be accessed in the GEO (Gene Expression Omnibus) DataSets with accession number GSE59811 (http://www.ncbi.nlm.nih.gov/geo/query/acc.cgi?acc=GSE59811).